Fermi National Accelerator Laboratory

Effects of Multiple Interactions and Pileup on the W Mass Measurement in the Electron Channel at D∅ in Run II and TeV33

Ashutosh V. Kotwal

For the DØ Collaboration

Fermi National Accelerator Laboratory
P.O. Box 500, Batavia, Illinois 60510

February 1997

Disclaimer

Distribution

Effects of Multiple Interactions and Pileup on the W Mass Measurement in the Electron Channel at DØ in Run II and TeV33

Ashutosh V. Kotwal

Department of Physics, Columbia University, New York, NY 10027, U.S.A.

ABSTRACT

At the DØ experiment the W mass has been measured in the electron channel using the calorimetric measurements of the electron's transverse energy and the transverse energy of the hadronic system recoiling against the W boson. We discuss the effects of multiple interactions and pileup on the biases and resolutions of the calorimetric energy measurements and on the W mass measurement in Run II and TeV33.

I. INTRODUCTION

The mass of the W boson is an important parameter of the Standard Model. The precise measurement of the W mass is one of the objectives of the physics program for the high luminosity running at the Fermilab Tevatron. At the DØ experiment, the W mass has been measured in Run 1 in the electron decay channel by using the calorimetric energy measurements of the decay electron and the hadronic recoil of the W. In this paper, we discuss the implications of running at high luminosity for the calorimetric measurements at DØ, and the resulting biases and resolutions in the W mass measurement.

The DØ detector has been described elsewhere [1]. The electron energy is measured in a 0.5×0.5 $\eta - \phi$ window (25 towers each of 0.1×0.1 area in $\eta - \phi$). In longitudinal depth the electron towers include the four readout sections of the electromagnetic calorimeter and the first readout section of the hadronic calorimeter. The hadronic recoil is measured using all calorimeter cells except the electron cells, a correction being applied for the recoil energy absorbed by the electron. We assume that these algorithms which are currently being used for the W mass measurement in Run 1 will also be used in Run II and TeV33.

II. CALORIMETER ELECTRONICS

The ionization electrons produced by the charged particles traversing the 2.3 mm liquid argon gap in the calorimeter cells drift across the gap in 430 ns. A charge-sensitive preamplifier connected to each calorimeter cell integrates the resulting triangular current pulse. In the Run II upgraded detector, a Sallen-Key high-pass filter will shape the preamplifier output to yield a voltage pulse which peaks 400 ns after the start of the detector current pulse, and falls rapidly afterwards. The peak amplitude is proportional to the integral of the current pulse, i.e. the total ionization charge. The peak amplitude from each crossing is sampled and stored on an array of capacitors (Switched Capacitor Array). Slowly varying offsets are measured by sampling the Sallen-Key output at the end of the superbunch gap, and are subtracted from subsequent readings. The Level1 trigger picks out the crossing that produced the interesting event, and

the baseline-subtracted voltage from the corresponding capacitor is read out.

The SPICE circuit simulation program is used to compute the shape of the Sallen-Key output for a triangular current pulse input to the preamplifier. Using the circuit of the Run II prototype, the output shown in figure 1 is obtained.

III. TEVATRON BUNCH STRUCTURE

We assume the following Tevatron bunch structure in Run II and beyond. One revolution around the Tevatron will consist of three superbunches of protons and antiprotons. Each superbunch will consist of a number of bunches spaced uniformly in time. Between the last bunch in a superbunch and the first bunch of the next superbunch will be a "gap" of 2.2 μs. At the start of Run II, each superbunch will consist of 12 bunches, corresponding to 396 ns between bunch crossings. As Run II progresses the number of bunches per superbunch will be increased to 36 to yield higher luminosity (132 ns between bunch cross-
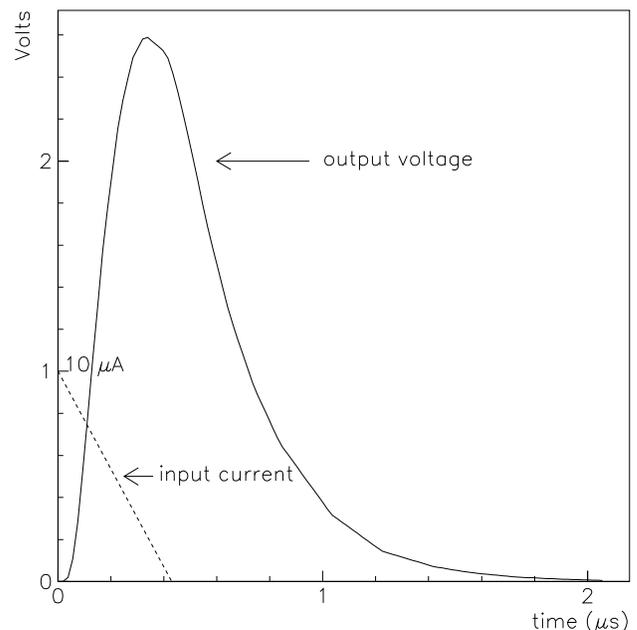

Figure 1: Output voltage pulse of the Run II calorimeter preamplifier and Sallen-Key filter combination for a triangular current pulse input.

ings). We will also explore a hypothetical situation for TeV33 with 126 bunches per superbunch.

IV. MONTE CARLO TECHNIQUE FOR ESTIMATING EFFECTS OF MULTIPLE INTERACTIONS AND PILEUP

Due to the shape of the Sallen-Key output, the peak magnitude is sensitive to the signals produced by the calorimeter cell before and after the crossing of interest. The distortion of the signal read from the crossing of interest due to the "out-of-time" signals, caused by the memory of the electronics, is called pileup. In addition to pileup, secondary interactions occurring in the same crossing that produced the W event also deposit energy in the calorimeter cells and distort the W event observables.

The pileup and instantaneous effects of the additional interactions are simulated in the following manner in a simple Monte Carlo program. We initialize the history of a large number of crossings by picking according to a Poisson distribution the number of minimum bias interactions occurring in each crossing. The average number of minimum bias interactions is calculated according to the chosen luminosity setting and the time between bunch crossings. For each minimum bias interaction, the transverse energy flow into the electron window and the hadronic recoil smearing vector is generated according to the distributions described below. The total for each crossing is cal-

culated by summing over the interactions.

The W event is now generated in a given crossing. The energies generated in all previous crossings are used to weight the electronics response curve from each crossing, appropriately delayed. The current crossing and the future crossings occurring within 400 ns are also considered. The sum of the magnitudes of the weighted and delayed response curves at the current time yields the pileup contribution. The baseline for each superbunch is calculated similarly. The changes in the W event observables on an event-by-event basis are histogramed to extract the mean biases and the resolutions.

V. W PRODUCTION AND DECAY MODEL

The angular distribution of the decay leptons in the W rest frame produces the characteristic Jacobian edge in the lepton transverse momentum (p_t) or transverse mass (m_t) spectrum. The edge corresponds to the case where the lepton decay axis is perpendicular to the beam axis. Since the position of the edge carries the maximum information about the W mass, for simplicity we simulate the bias and smearing of the Jacobian edge only. We also take the simple case of full angular acceptance, hence the longitudinal momentum of the W does not affect the transverse momentum spectra of the decay leptons. We generate W's with no longitudinal momenta. We assume a true W mass of 80 GeV, so that the true electron p_t is 40 GeV and the true transverse mass is 80 GeV in the W rest frame. Finally, we generate the transverse momentum of the W according to the calculation of Ladinsky and Yuan [2], which includes the perturbative, resumed and non-perturbative components of the W p_t spectrum. The W p_t is restricted to be below 30 GeV, following the DØ Run 1 W mass analysis. The W p_t spectrum is shown in figure 2. In the rest frame of the W, the direction of the W p_t is generated randomly in ϕ with respect to the direction of the electron p_t.

VI. E_T AND $\not{E}_t$ MODEL FOR MINIMUM BIAS INTERACTIONS

We will study the electron p_t and the transverse mass since both are interesting from the point of view of extracting the W mass.

Each minimum bias interaction produces some transverse energy flow into the 0.5×0.5 $\eta - \phi$ electron window. We measure the mean transverse energy per minimum bias interaction overlapping the electron from the DØ Run 1 data. The dependence of the mean transverse energy on luminosity is shown in figure 3. Since an instantaneous luminosity of $5.7 \times 10^{30}/\text{cm}^2/\text{s}$ produces an average of one interaction per crossing in Run 1 (assuming a minimum bias cross-section of 50 mb), the fitted slope in figure 3 converts to a bias in the electron p_t of 64 MeV/interaction. This quantity is assumed to be independent of the pseudorapidity η. The spectrum is taken according to the form fitted by CDF to their data [3]

$$d\sigma/dp_t^2 \sim 1/(p_0 + p_t)^{8.26} \qquad (1)$$

where p_0 is adjusted so that $< p_t > = 64$ MeV.
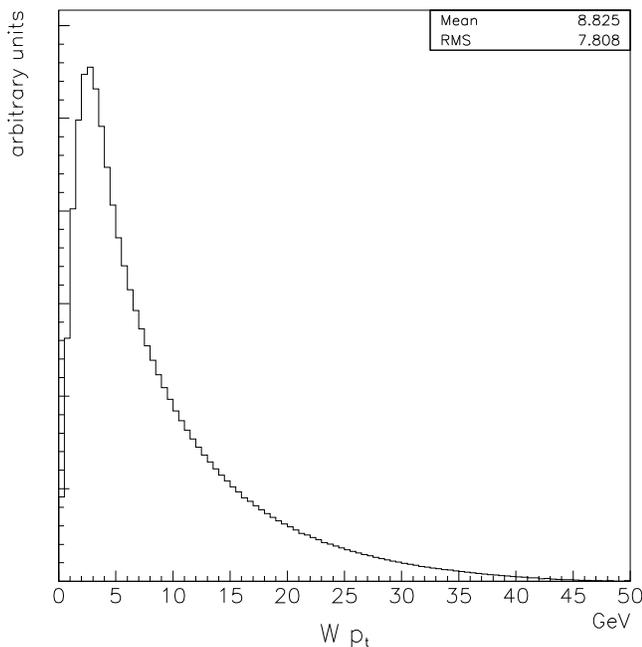

| Mean | 8.825 |
| RMS | 7.808 |

Figure 2: Transverse momentum spectrum of W, according to the calculation of Ladinsky and Yuan.

The minimum bias interactions also smear the measurement of the hadronic recoil. The missing transverse energy ($\not{E}_t$) vector measured in minimum bias interactions, which is distributed randomly in ϕ with respect to the recoil direction, smears the magnitude and direction of the recoil momentum vector. The $\not{E}_t$ distribution measured from low instantaneous luminosity minimum bias events in DØ Run 1 data is shown in figure 4. By studying the dependence of the $\not{E}_t$ distribution on instantaneous luminosity, we conclude that each minimum bias event contributes 1.68 GeV to the resolution in $\not{E}_x$ and $\not{E}_y$ (z is the beam direction). The distributions of $\not{E}_x$ and $\not{E}_y$ are approximated quite well by Gaussians.

We simulate the intrinsic electromagnetic calorimeter resolution and the underlying event, which affect the measurement of the W observables even in the absence of additional interactions. These effects set an irreducible floor in the biases and resolutions. We simulate the stochastic resolution of the electron E_t measurement as $13.5\%/\sqrt{E_t}$, as measured using the DØ test beam data. We also simulate the contribution to the electron E_t resolution of 1% due to systematic effects (constant term), as measured using the observed width of the Z^0 in DØ data. The recoil p_t resolution is modelled as $4\% \oplus 50\%/\sqrt{p_t}$, where the constant term is measured from test beam and jet data, and the sampling term is determined from Z^0 p_t balance [4].

The underlying event produced by the spectator quark interactions produces energy flow into the calorimeter electron window. We measure the distribution of the transverse energy added to the electron from low p_t W events. The measured distribution shown in figure 5 is used to simulate this energy flow, including the noise contribution. The underlying event also smears the hadronic recoil measurement. Analysis of the Z^0 p_t balance shows that the underlying event acts like one minimum bias interaction accompanying the boson production [4]. The $\not{E}_t$ distribution shown in figure 4, which represents the superposition of one minimum bias event and detector noise, is used to simulate the underlying event.

VII. SIMULATION RESULTS

We start with the typical Run II scenario, when the instantaneous luminosity is $2 \times 10^{32}/\text{cm}^2/\text{s}$, and each superbunch consists of 36 bunches. The average number of additional minimum bias interactions per crossing is 1.94. We first look at the fractional change in the electron E_t and the transverse mass produced by all the simulated effects for W's produced with zero transverse momentum. The distributions of the fractional change are shown in figure 6. The bias and the resolution on $E_t(e)$ and m_t depend on which bunch in a superbunch produced the W event. Figures 7 and 8 show these dependences. The first and last few bunches in a superbunch suffer from reduced pileup effects because the calorimeter integrates over fewer (past or future) crossings.

We now study the luminosity dependence of the mean bias and resolution in $E_t(e)$ and m_t. We have chosen four luminos-
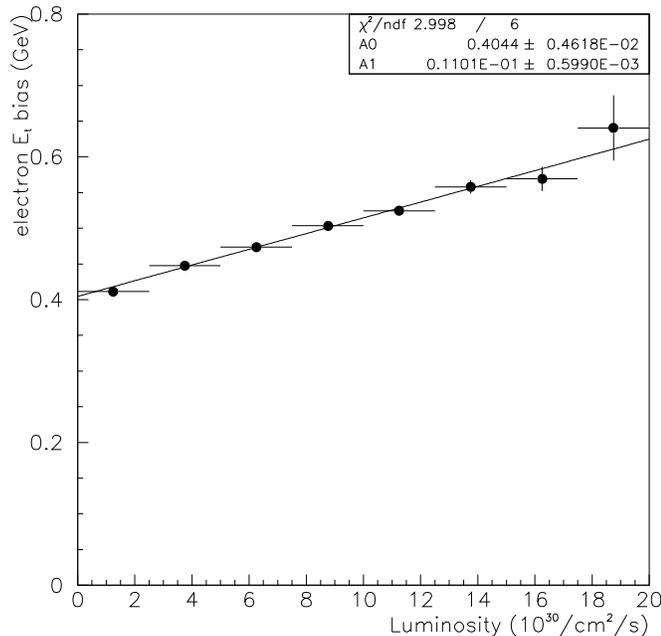
Figure 3: Luminosity dependence of the transverse energy flow due to additional interactions, measured in the electron window.
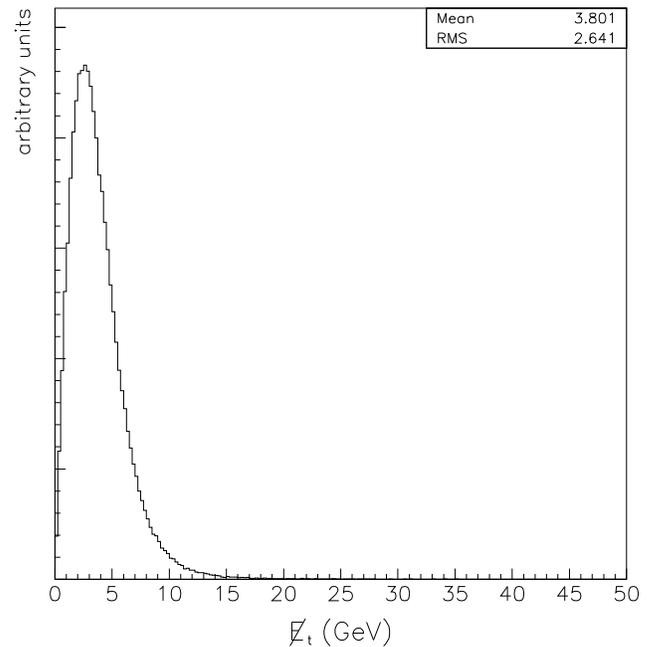
Figure 4: $\not{E}_t$ distribution measured in minimum bias triggers at low luminosity.

ity settings of 0.01, 0.4, 2 and 10 in units of $10^{32}/\text{cm}^2/\text{s}$, selected to represent a low luminosity setting, the estimated initial and default Run II settings, and TeV33 respectively. For 36 bunches/superbunch (132 ns/crossing), these luminosities correspond to an average of 0.001, 0.39, 1.94, and 9.7 additional interactions per crossing respectively. The luminosity dependence of the $E_t(e)$ and m_t bias and resolution is shown in figures 9 and 10 respectively, for W's produced with and without transverse momentum.

We study the dependence of the bias and resolution on the bunch structure. We consider the case of 12 bunches/superbunch (396 ns/crossing), which will exist in the initial stages of Run II, and a hypothetical case of 126 bunches/superbunch (38 ns/crossing), to approximate the effect of a higher frequency Tevatron RF. To first approximation, we expect that at a fixed luminosity the calorimeter integrates the signals from the same number of interactions, regardless of the bunch crossing time. Hence the pileup effects do not depend strongly on the bunch crossing time. With reduced crossing time we expect a small reduction in the pileup effects because the electronics response is most sensitive to the in-time interactions due to the peaking of the response curve. Hence by spreading out the interactions in time we slightly reduce the pileup effects. Figures 11 and 12 show the luminosity dependence of the biases and resolutions for each of the three bunch structures. Here we have ignored the p_t of the W. While there is marginal reduction in the biases and improvement in the resolutions as we change from 396 ns to 132
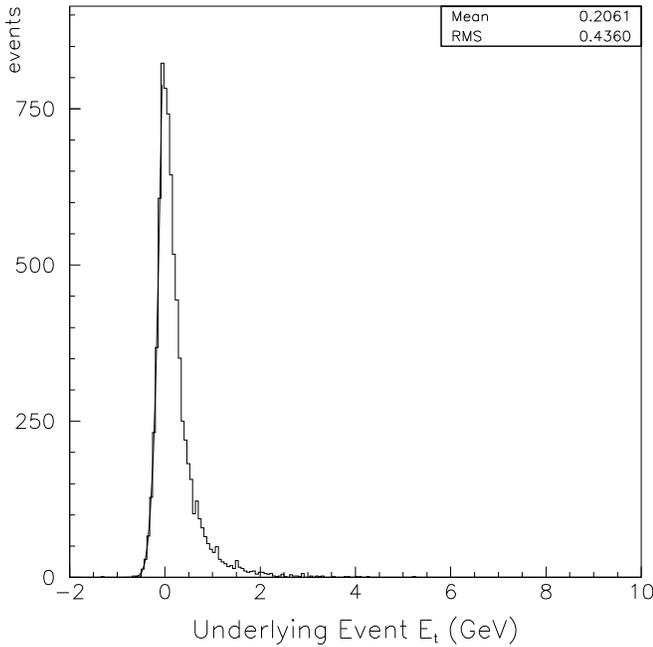
ns bunch-crossing time (at constant luminosity), there is negligible change with further reduction in crossing time below 132 ns.

Finally, we note that the effect of the transverse energy flow from minimum bias events on the electron E_t resolution depends on the shape of the distribution of the minimum bias E_t. As a check, we replace our model given in equation 1 with two other simple models, one given by an exponential in p_t^2 and another given by an exponential in p_t. The slope parameter in these models is tuned to give a mean of 64 MeV. For the case of 132 ns crossing time and zero W p_t, the electron E_t resolution predicted using the three models is shown in figure 13. The size of the fluctuations in the E_t flow is different for these models, however the differences are small compared to the intrinsic resolution of the calorimeter. Hence the electron E_t resolution at 40 GeV is not sensitive to the detailed shape of the minimum bias E_t distribution.

VIII. PHYSICS IMPLICATIONS

The salient features of these results are governed by the magnitude of the minimum bias E_t and the number of minimum bias interactions that are integrated by the calorimeter (N_{int}). The

Figure 5: Measured distribution of the transverse energy overlapping the electron produced by the underlying event.
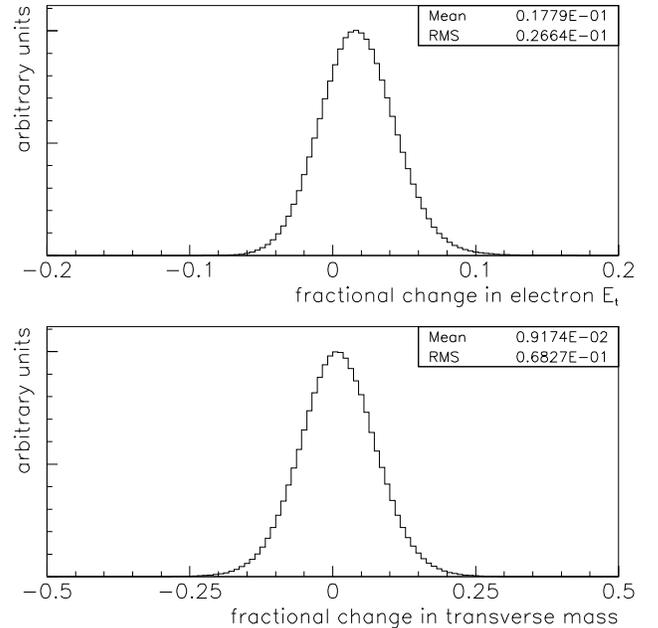

Figure 6: Distributions of fractional change in $E_t(e)$ and transverse mass caused by multiple interactions, underlying event and calorimeter resolution. W's were generated with zero transverse momentum. These simulations correspond to a luminosity of $2 \times 10^{32}/\text{cm}^2/\text{s}$ with 36 bunches/superbunch, producing an average of 1.94 additional minimum bias interactions per crossing.
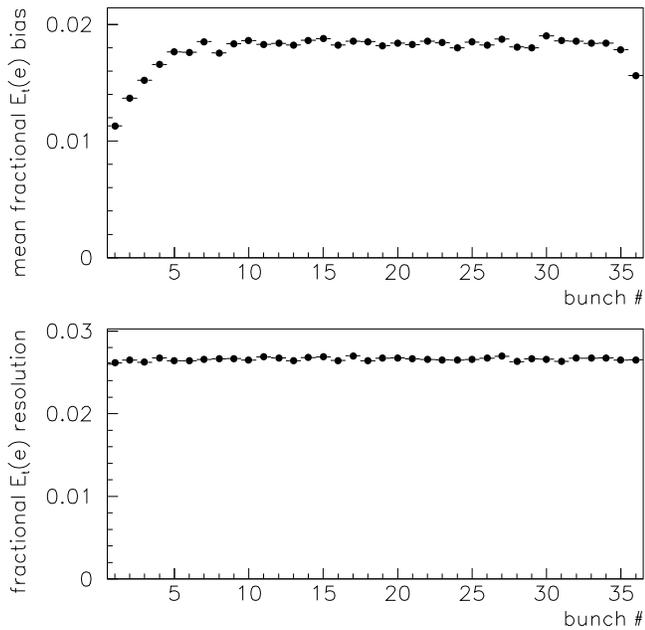
Figure 7: Dependence of the fractional bias and resolution in electron E_t on the sequential bunch number in the superbunch. W's were generated with zero transverse momentum. These simulations correspond to a luminosity of 2×10^{32}/cm²/s with 36 bunches/superbunch, producing an average of 1.94 additional minimum bias interactions per crossing.
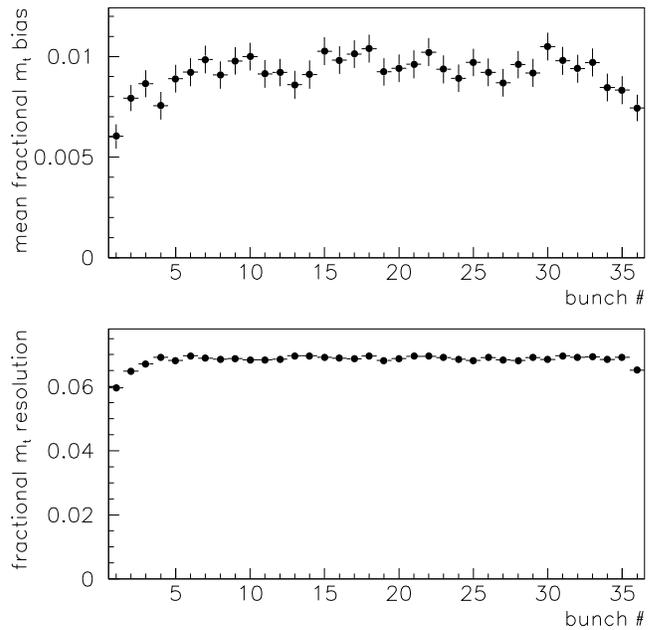
Figure 8: Dependence of the fractional bias and resolution in transverse mass on the sequential bunch number in the superbunch, for the same conditions as in figure 7.

bias in the electron E_t is 64 MeV/interaction, and we may assume the fluctuations are of the same order. The smearing in the recoil p$_t$ is ∼2.4 GeV. The electron E_t bias increases linearly with N_{int}, while the smearing in E_t(e) and m$_t$ increases as $\sqrt{N_{int}}$. At the four luminosity settings we have considered, an average of 0.03, 1.2, 5.8 and 29 minimum bias interactions respectively occur during the 400 ns charge integration time [1].

We consider the statistical power of the transverse mass fit. The transverse mass resolution is dominated by the smearing of the recoil vector due to the fluctuations in the underlying event and the additional interactions. At Run II luminosities the smearing vector approaches the recoil vector in magnitude. At higher luminosities the smearing vector dominates and the measurement of the recoil is severely degraded. Since the m$_t$ resolution is degrading as $\sqrt{N_{int}}$, further increases in instantaneous luminosity produce diminishing reductions in the W mass statistical error from the m$_t$ fit.

We consider the statistical power of the electron E_t fit. At the nominal TeV33 luminosity, the fluctuations in the minimum

bias E_t flow cause a spread in the electron E_t of ∼350 MeV or ∼1%. The electron E_t resolution is dominated by the intrinsic calorimeter resolution. The smearing of the Jacobian edge is dominated by the W p$_t$, which is ∼10%. Hence the statistical power of the electron E_t fit is independent of instantaneous luminosity, and we expect the statistical error of the W mass measurement to scale as the inverse square root of the number of events ($1/\sqrt{N_{ev}}$ scaling) in Run II and TeV33.

Simulations have shown that a sample of 30000 events (similar to the actual DØ Run1b sample) gives a statistical error on the W mass of 67 MeV from the transverse mass fit and 100 MeV from the electron E_t fit. These estimates are in agreement with the preliminary W mass analysis of the DØ Run1b data [4]. We show estimates of the statistical precision of the W mass measurement for Run 1b, Run II and TeV33 in table I.

Estimating the total uncertainty requires further assumptions. Run 1 analyses have shown that most of the inputs to the measurement are constrained by the collider data, so that the systematic uncertainties also scale as $1/\sqrt{N_{ev}}$. Assuming scaling of systematic uncertainties at higher luminosity, we estimate 34 MeV uncertainty from the transverse mass method for Run II. The factor of two between total uncertainty and statistical uncertainty is obtained from the DØ Run 1a analysis [5]. Similar scaling to TeV33 leads to an estimate of 26 MeV for the total W mass uncertainty with the m$_t$ method.

If we assume the same factor of two for the electron E_t

Table I: Estimated Statistical Precision of W Mass Measurement.

Run	Instantaneous Luminosity	Integrated Luminosity	W event sample	ΔM_W (m_t fit)	ΔM_W (E_t(e) fit)
Run1b	7.4×10^{30}/cm²/s	76/pb	3×10^4	67 MeV	100 MeV
Run II	2×10^{32}/cm²/s	2/fb	8×10^5	17 MeV	19 MeV
TeV33	1×10^{33}/cm²/s	10/fb	4×10^6	13 MeV	9 MeV

method, we can estimate a total uncertainty of 38 MeV for Run II and 18 MeV for TeV33. If we assume that the E_t(e) method achieves the same total uncertainty as the m_t method at low luminosity, then the scale factor is reduced to 1.4. We then estimate an uncertainty of 27 MeV for Run II and 13 MeV for TeV33 using the E_t(e) method.

We must also consider the mean bias introduced in electron E_t by the transverse energy flow produced by the additional interactions. According to figure 9, we expect ∼7% shift in the electron E_t at TeV33 (the fractional shift in m_t being half the fractional shift in E_t(e)). If the mean shift is measured from the data, then the error on the mean, which scales as $\sqrt{N_{int}/N_{ev}}$, will remain constant as instantaneous luminosity increases. From figure 3 we see that the fitted slope, and therefore the mean bias of 64 MeV/interaction, is measured to 5.5% of itself from the Run 1b W data. This contributes an uncertainty of 3.5

the mean shift does not become a large fraction of the total W mass uncertainty in a high precision measurement.

IX. CONCLUSIONS

We have estimated the effects of multiple interactions and pileup on the DØ W mass measurement using Run II Upgrade calorimetry at high luminosities. The mean biases and resolutions affecting the transverse mass fit and the electron transverse momentum fit have been calculated using the simulated response of the Run II Upgrade electronics and properties of minimum bias events measured from data. The estimates are based on the use of measurement techniques and algorithms similar to those currently being used in Run 1.

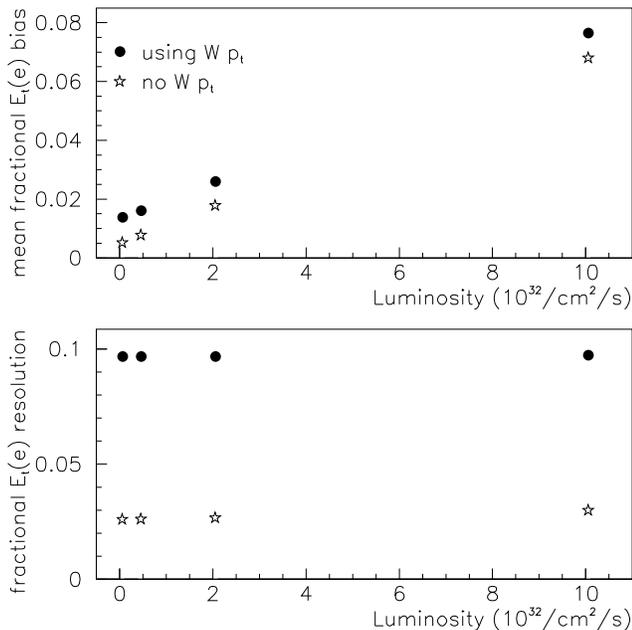We estimate a statistical uncertainty of 17 MeV on the W mass

Figure 9: Luminosity dependence of the fractional bias and resolution in electron E_t.
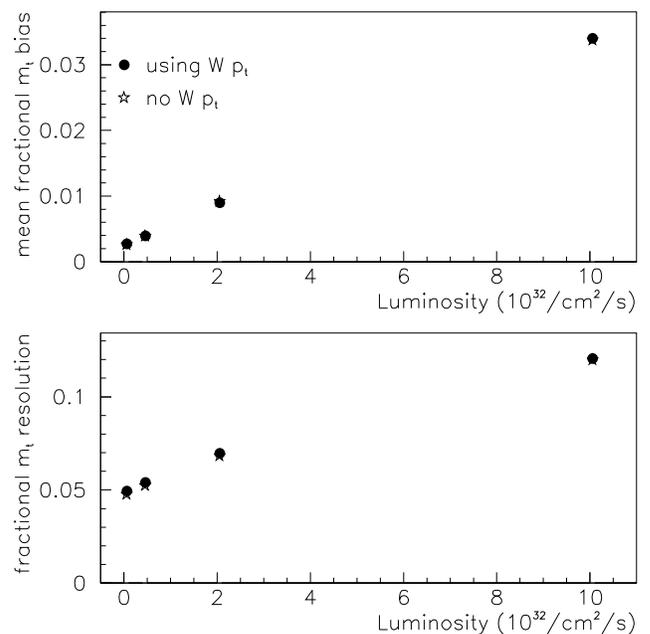

Figure 10: Luminosity dependence of the fractional bias and resolution in transverse mass.

for a Run II measurement using the transverse mass method. This reduces to 13 MeV for TeV33. The statistical precision does not scale as $1/\sqrt{N_{ev}}$ because of the degrading resolution of the W p_t measurement. If the total uncertainty continues to be twice the statistical uncertainty, a precision of 34 MeV (26 MeV) on the W mass measurement using the transverse mass method may be achieved in Run II (TeV33).

The electron p_t method can achieve a statistical precision of 19 MeV and 9 MeV for Run II and TeV33 respectively. Optimistically, this method could achieve a total W mass uncertainty of 27-38 MeV for Run II and 13-18 MeV for TeV33.

X. REFERENCES

[1] DØ Collaboration, S. Abachi *et al.*, Nucl. Instrum. Meth. **A338**, 185-253 (1994).

[2] G. A. Ladinsky and C. P. Yuan, Phys. Rev. **D50**, 4239 (1994).

[3] CDF Collaboration, F. Abe *et al.*, Phys. Rev. Lett. **61**, 1819 (1988).

[4] *W Boson Mass Measurement using Run 1b Data,* I. Adam, E. Flattum, U. Heintz, A. V. Kotwal, Internal DØ Note, May 1996 (unpublished).

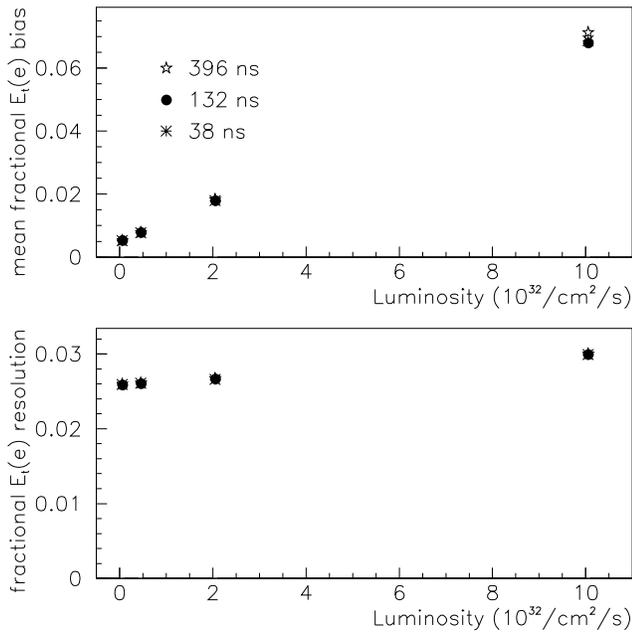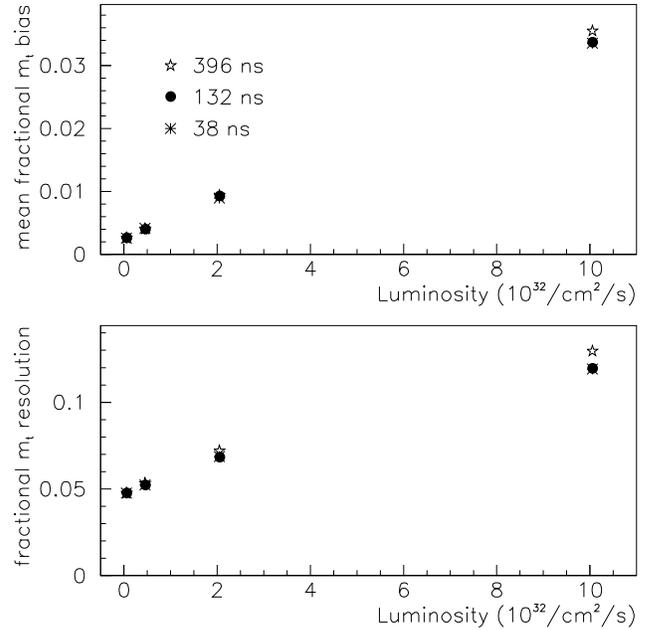[5] DØ Collaboration, S. Abachi *et al.*, Phys. Rev. Lett. **77**, 3309 (1996).

Figure 12: Luminosity dependence of the fractional bias and resolution in transverse mass for 12, 36 and 126 bunches/superbunch respectively. W's were generated with zero transverse momentum.
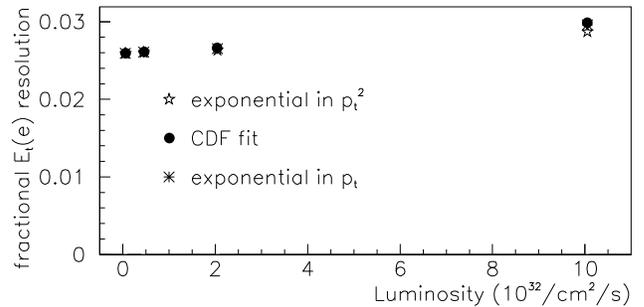

Figure 11: Luminosity dependence of the fractional bias and resolution in electron E_t for 12, 36 and 126 bunches/superbunch respectively. W's were generated with zero transverse momentum.

Figure 13: Dependence of the predicted E_t(e) resolution on the minimum bias E_t model, for 36 bunches/superbunch. W's were generated with zero transverse momentum.